Ultrasound Doppler Measurements of Low Velocity Blood Flow: Limitations Due to Clutter Signals from Vibrating Muscles

Andreas Heimdal, *Student Member, IEEE,* and Hans Torp, *Member, IEEE*

***Abstract*—Skeletal muscles vibrate under sustained contraction, and generate low frequency side band clutter in the doppler signal. Both shivering in the hand of the operator and muscle vibrations in the patient itself give rise to the clutter. Clutter rejection filters are commonly used to remove the low frequency components, but the doppler signal from low velocity blood flow is then also lost. This paper describes a model for the pulsed wave (PW) doppler signal from vibrating muscles, reviews a model for the PW doppler signal from moving blood, and by comparing these models presents a theoretical minimum for detectable blood velocity in small vessels, being typically 6.4 mm/s for 6 MHz doppler. The limit has a nonlinear relation to the ultrasound frequency. The model also shows that the radial component of the muscle vibrations can be estimated from the phase of the doppler signal.**

I. Introduction

Skeletal muscle tension is known to oscillate involuntarily under sustained contraction [1]. This is caused by the mechanism for maintaining contraction which is based on repetitive nervous stimulation of the muscle. Increased force is achieved by increased stimulation frequency. The vibrations produce low frequency sound, and frequencies in the range 5 to 36 Hz have been reported [2], [3]. The sound intensity has been found to be proportional to the load on the muscle. The heart muscle does not vibrate in the same manner, but vibrations in the surrounding tissue when the heart valves open and close, as well as oscillations in the valve leaflets themselves are reported [4], [5].

The detection of low velocity blood flow with ultrasound doppler techniques is limited by *clutter noise*. The doppler signal spectrum from a perfectly still target will have only a DC component. A vibrating target will introduce low frequency side bands around this DC component. Vibrating muscles in the hand of the operator holding the ultrasound probe, as well as vibrating targets in the imaged region of the patient itself will introduce this low frequency side band noise. Traditionally, clutter noise has been considered to arise mainly from vessel wall motion and gross tissue motion. The effect of this motion is a frequency shift of the DC component and the side bands in the signal spectrum according to the doppler equation. The lower limit for blood flow detection is thus a sum of the velocity corresponding to the bandwidth of the vibration clutter and the velocity of the tissue motion. In peripheral and coronary arteries the vessel wall can have velocities up to 5 mm/s [6], while the gross tissue motion in the myocardium can have velocities up to 55 mm/s [7, p. 133]. The effect of the clutter noise can be reduced by minimizing the size of the sample volume [8], but even when the whole sample volume is inside a blood vessel, vibration clutter noise from reverberations and side lobes can dominate the signal.

Low velocity blood flow occurs mainly in the capillaries. During resting conditions, the average velocity is 0.33 mm/s [9]. The skin capillary blood cell velocity has for instance been measured to 0.60 ± 0.51 mm/s [10]. Measuring capillary blood flow is of great clinical value since the efficiency of the exchange of nutrients between blood and tissue is given by this flow. Measuring the low velocity blood flow in tumor vessels is also a field of current interest [11], [12]. Low average velocities are also found in venules, small veins, arterioles, and small arteries, with 3.3 mm/s, 10 mm/s, 20 mm/s, and 40 mm/s, respectively [9]. The mean flow velocity of the dorsal pedal artery is for instance 34 ± 16 mm/s .

The weakest detectable echo from blood can, depending on the dynamic range of the ultrasound scanner, be more than 100 dB weaker than the echo from tissue. To detect the low amplitude blood signal, clutter rejection filters that suppress the strong low frequency components from the tissue movements are commonly used. A better design of the rejection filters will be possible given better knowledge of the clutter signal that is supposed to be removed. In this paper a model for the clutter signal from vibrating muscles is presented and a model for the doppler signal from moving blood is reviewed. By comparing these models we present a table of the theoretically minimum detectable blood velocities at different ultrasound frequencies.

II. Doppler Signal Models

In pulsed wave (PW) doppler, several pulses are fired in the same direction at a rate given by the pulse repetition frequency (PRF). By demodulating and sampling the echo signal from each pulse at the same lag $\tau_{SV} = 2r_{SV}/c$, where

Manuscript received June 28, 1996; accepted February 25, 1997. This work was supported by the Norwegian Research Council.

The authors are with Department of Physiology and Biomedical Engineering, Faculty of Medicine, Norwegian University of Science and Technology, Trondheim, Norway (e-mail: andreash@medisin.ntnu.no).

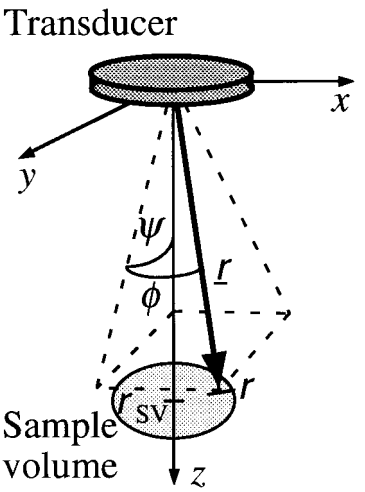

Fig. 1. The spatial coordinates used in the doppler signal model.

c is the speed of sound, one can construct the *complex doppler signal* from a small sample volume (SV) at distance r_{SV} from the transducer:

$$x(t) = \alpha \int_{\mathrm{SV}} s(\tau_{\mathrm{SV}} - 2r/c) e^{i(\omega_0 \tau_{\mathrm{SV}} - 2k_0 r)} B(\underline{r}) v(\underline{r}, t) d\underline{r}. \tag{1}$$

Here the integration is performed over the sample volume in the spatial co-ordinates $\underline{r}(r, \phi, \psi)$, as shown in Fig. 1. In the model, $s(t)$ is the complex envelope of a received pulse from a point scatterer, $B(\underline{r})$ is the two-way beam profile, describing the spatial sensitivity of the transducer, $v(\underline{r}, t)$ is the scattering fluctuation, $k_0 = \omega_0/c$ is the wave number, ω_0 is the angular center frequency of the pulse, and α is a constant combining the attenuation, gain, and receiver sensitivity. The signal is a function of time after the first fired pulse. Since each pulse is sampled only once in the sample volume, only the discrete samples $x(t = mT)$ of the signal are available, where $T = 1/\mathrm{PRF}$ is the time between each pulse.

A. Vibration Clutter Signal Model

To model the complex doppler signal from vibrating tissue we assume that the imaged tissue can be approximated with point scatterers randomly distributed in the sample volume, and that all the scatterers have uniform motion. The position of scatterer number n is then described by:

$$\underline{r}_n(t) = [r_n - d_r(t)]\underline{e}_r + [\phi_n - d_\phi(t)]\underline{e}_\phi + [\psi_n - d_\psi(t)]\underline{e}_\psi \tag{2}$$

where $\underline{e}_r$, $\underline{e}_\phi$, and $\underline{e}_\psi$ are the unit vectors in the radial, lateral (in the scan plane), and elevation directions, respectively. The scatterer mean positions (r_n, ϕ_n, ψ_n) are randomly distributed in the sample volume, while the zero mean displacement functions $d_r(t)$, $d_\phi(t)$, and $d_\psi(t)$ are equal for all the scatterers. This means that no deformation of the tissue is included in the model. This is reasonable when vibrations of the probe itself dominate, or when the sample volume is small compared to the size of the muscle. The three displacement functions are also assumed to have the same frequency components.

With point scatterers as described in (2), the scattering fluctuation function is a sum of Dirac delta functions:

$$v(\underline{r}, t) = \sum_n \delta(\underline{r} - \underline{r}_n(t)) \tag{3}$$

and the complex doppler signal becomes

$$x(t) = \alpha \sum_n s(\tau_{\mathrm{SV}} - 2(r_n - d_r(t))/c) e^{i(\omega_0 \tau_{\mathrm{SV}} - 2k_0(r_n - d_r(t)))} \times B(r_n - d_r(t), \phi_n - d_\phi(t), \psi_n - d_\psi(t)) \tag{4}$$

which is recognized as a sum of signals that are simultaneously *phase modulated* (PM) with a function of the radial component of the movement, and *amplitude modulated* (AM) with the pulse envelope function $s(n, t)$ and the beam profile function $B(n, t)$ which together have all the spatial components of the movement as arguments.

AM signals have a bandwidth equal twice the maximum frequency of the modulating signal. Because PM signals in addition have an infinite number of side-bands, the phase modulation will give larger bandwidth than the amplitude modulation. In a practical situation there will always be additive white noise present. Since only a limited number of the side-bands are above the noise floor, a practical PM bandwidth can be found. A bandwidth requirement used for transmission of a PM signal over a radio channel is given by *Carson's rule* [14]:

$$W \approx 2\Delta f \left(1 + \frac{1}{\beta}\right) \tag{5}$$

where the *frequency deviation* Δf is the maximum instantaneous frequency which in our case becomes

$$\Delta f = \frac{k_0}{\pi} \max_t \left(\frac{d[d_r(t)]}{dt}\right) \tag{6}$$

and the *modulation index* is

$$\beta = \Delta f / f_m \tag{7}$$

where f_m is the maximum frequency of the modulating signal $d_r(t)$. The modulation index represents the maximum phase deviation of the PM signal. Since the PM bandwidth is independent of the summation index n in (4), the total signal bandwidth will equal the PM bandwidth. A high dynamic range ultrasound clutter signal will have a higher bandwidth than given by (5).

A more thorough description of the frequency spectrum of the clutter signal in (4) can be found if we assume the amplitude of the motion is much smaller than the spatial size of the point spread function. This means that the value of the pulse envelope and the beam profile can be approximated as constant for each n, $s(n, t) = s_n$, and $B(n, t) = B_n$, which means the doppler signal can be written

$$x(t) = \alpha \left(\sum_n s_n B_n e^{i(\omega_0 \tau_{\mathrm{SV}} - 2k_0 r_n)}\right) e^{i2k_0 d_r(t)} = A e^{i2k_0 d_r(t)} \tag{8}$$

which is a PM signal modulated with the scaled radial displacement function $2k_0 d_r(t)$. The complex constant A gives the amplitude and mean phase lag of the signal.

As seen from (8), the radial displacement function can be found from the phase of the doppler signal

$$d_r(t) = \frac{1}{2k_0}[\arg(x(t)) - \arg(A)]. \tag{9}$$

In practice the DC component is removed from the signal through high pass filtering in the receiver, so the phase of the constant A must be estimated from the motion pattern of $x(t)$ in the complex plane, as described in the Appendix.

The Fourier spectrum of the vibration clutter signal can be analytically described for a single frequency radial displacement function

$$d_r(t) = a\cos(2\pi f_v t) \tag{10}$$

where a is the vibration amplitude, and f_v is the vibration frequency. Inserting this into (8) we get a single tone PM signal. The modulation index in (7) will in this case be

$$\beta = 2k_0 a. \tag{11}$$

The Fourier spectrum of the signal in (8) can be found to be [14]:

$$X(f) = A\sum_{n=-\infty}^{\infty} J_n(2k_0 a)\delta(f - nf_v) \tag{12}$$

where the J_n is the n'th order Bessel function of the first kind. The corresponding *clutter signal power spectrum* is

$$P_c(f) = |X(f)|^2 = |A|^2 \sum_{n=-\infty}^{\infty} J_n^2(2k_0 a)\delta(f - nf_v). \tag{13}$$

Sample power spectra for different values of β are given in Fig. 2. A frequency normalized to the vibration frequency f_v is used on the x-axes of the plots. For signals specularly reflected from vibrating targets the ultrasound frequency dependency of the amplitude factor A is negligible, while for volume scattering the frequency dependency varies [15].

$$|A(f_0)| \propto \begin{cases} f_0^0 = 1 & \text{Specular scattering} \\ f_0^p, \quad 0 < p < 2 & \text{Volume scattering} \\ f_0^2 & \text{Rayleigh scattering} \end{cases}. \tag{14}$$

The spectra of arbitrary radial displacement functions are more cumbersome to develop analytically, as the total spectrum is a convolution of the PM spectra for each frequency component in the displacement function. Still the bandwidth is restricted as in (5). Since the vibration usually is caused by several muscle groups working simultaneously, the radial displacement function is expected to be a narrowband signal rather than a single frequency signal. A numerical estimation of the spectrum can be found by simulating a band limited signal, inserting it in (8) and

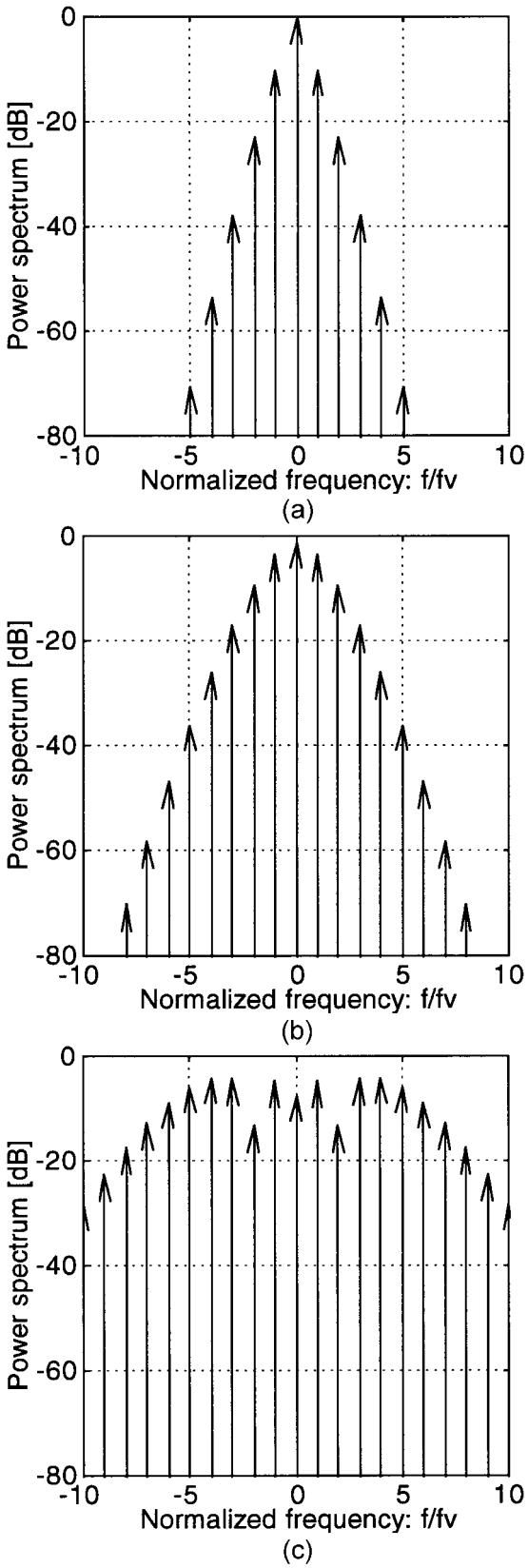

Fig. 2. Sample power spectra of a PM signal modulated with a single frequency modulating signal for varying modulation indices: (a) $\beta = 0.2$, (b) $\beta = 1$, (c) $\beta = 5$. The frequency axis is in each panel normalized to the vibration frequency.

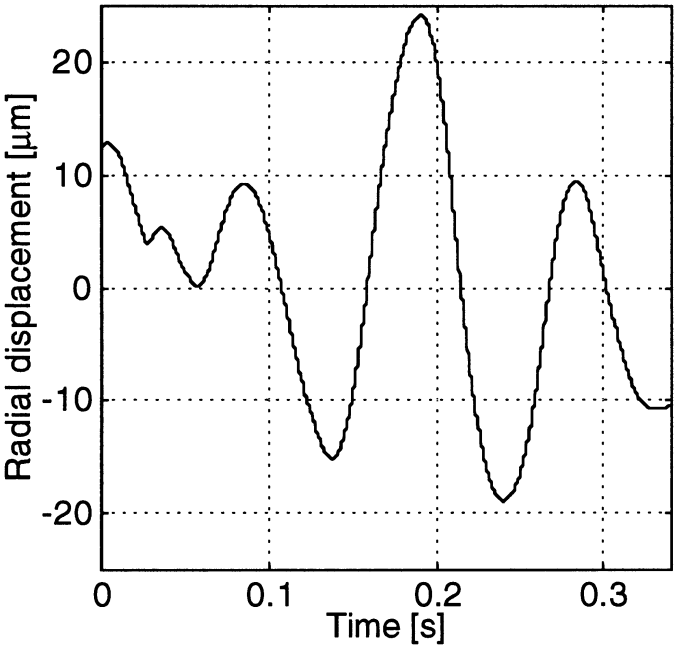

Fig. 3. The radial motion estimated from the doppler signal from a hand-held transducer and a fixed target. The corresponding vibration power spectrum is given in Fig. 4(a).

estimating the spectrum of the resulting doppler signal. For modulation indices $\beta \ll 1$, the exponential function in (8) can be estimated with $1 + i2k_0 d_r(t)$, indicating that the doppler signal has the same bandwidth as the displacement signal.

In color flow imaging, only short time segments up to 50 ms of the doppler signal are available. If the time segment is much smaller than $1/f_m$, which is the case for $f_m \ll 20$ Hz, the movement of the tissue is so slow that it appears to have an approximately constant velocity, and the doppler spectrum estimate gets a narrow frequency band centered around the doppler shift frequency.

B. Blood Signal Model

To obtain a simple model, blood flow with constant rectilinear velocity is considered. The velocity is in spherical components described by $\underline{\nu} = (\nu_r, r\nu_\phi, r\nu_\psi)$. The PW doppler signal from blood can be described using the same model as in (1) if the scattering fluctuation is defined as $v(\underline{r}, t) = v_a n(\underline{r}, t)$, where $n(\underline{r}, t)$ is the local concentration of red blood cells, and v_a is a scaling factor [16]. The cell concentration can be assumed to be delta-correlated in space. The backscattering will then be in the form of Rayleigh scattering, and the amplitude constant α will have the following ultrasound frequency dependency [17]:

$$\alpha = \alpha_b(f_0) = \alpha_{b0} f_0^2. \tag{15}$$

A simple model for the autocorrelation function of the

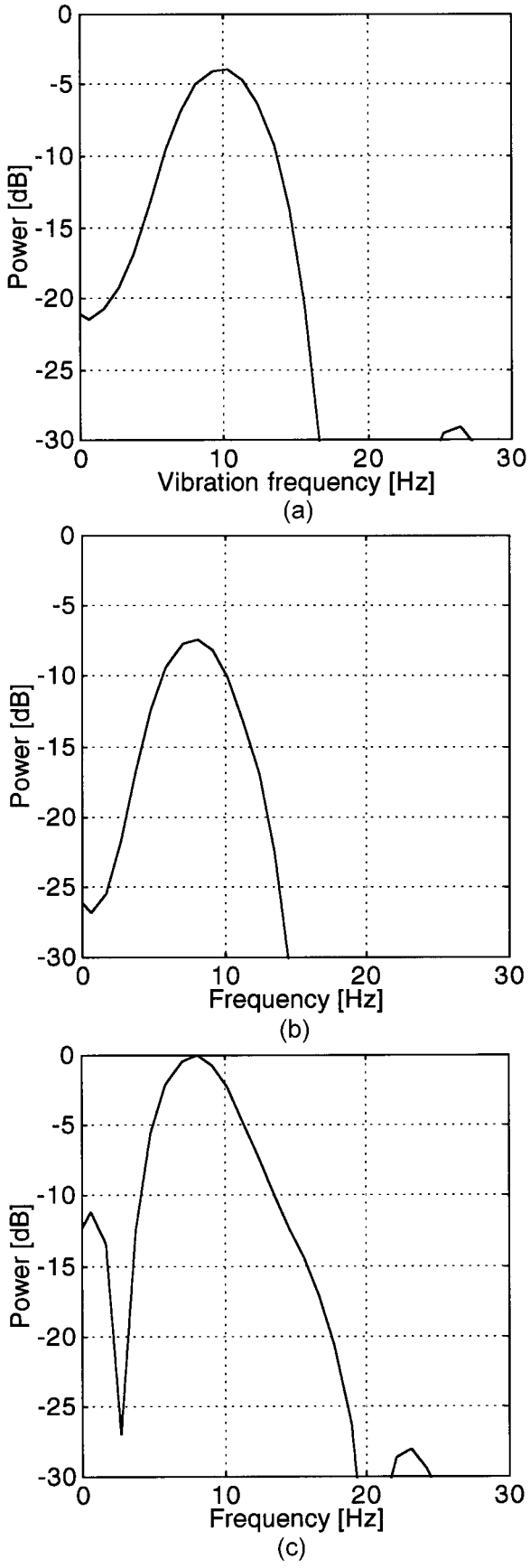

Fig. 4. Power spectra of the radial displacements for (a) a fixed target and a hand-held probe, (b) a relaxed biceps muscle and a fixed probe, and (c) a strained biceps muscle and a fixed probe.

doppler signal from blood is [16]:

$$R(\tau) \approx \alpha_b^2 \exp\left(-\frac{3(\nu_r\tau)^2}{2L^2} - \frac{3(\nu_\phi\tau)^2}{2\Theta^2} - \frac{3(\nu_\psi\tau)^2}{2\Theta^2} + i2k_0\nu_r\tau\right) \quad (16)$$

where L is the pulse length, and Θ is the -3.25 dB beam opening angle. The ultrasound frequency dependencies of these two parameters are [15]:

$$\begin{aligned} L(f_0) &= N_p\frac{c}{f_0} \\ \Theta(f_0) &= \frac{c}{f_0 D} \end{aligned} \quad (17)$$

where N_p is the number of periods in the pulse burst, and D is the transducer diameter. The blood signal power spectrum is found as the Fourier transform of the autocorrelation function to be

$$P_b(f) \approx \begin{cases} \alpha_b^2\left|\sqrt{\frac{\pi}{b}}\right| \exp\left(-\frac{\pi^2}{b}\left(f - 2f_0\frac{\nu_r}{c}\right)^2\right), & b > 0 \\ \alpha_b^2\delta\left(f - 2f_0\frac{\nu_r}{c}\right), & b = 0 \end{cases} \quad (18)$$

$$b = \frac{3}{2}\left(\frac{\nu_r^2}{L^2} + \frac{\nu_\phi^2}{\Theta_2} + \frac{\nu_\psi^2}{\Theta^2}\right).$$

III. Materials and Methods

A 6 MHz annular array transducer and a CFM-800 ultrasound scanner (Vingmed Sound AS, Horten, Norway) were used to collect ultrasound doppler data. In the scanner the doppler signal was quadrature demodulated, and the complex analog doppler signal, without fixed target canceling (FTC), was transferred to a Macintosh computer as a stereo audio signal and digitized with 12 bits at 44 kHz. The computer audio input was band limited 10 Hz to 19 kHz, so the DC component of the doppler signal had to be estimated as described in the Appendix. The digitized signal was decimated to 4.4 kHz for memory reasons. MATLAB was used for signal processing in the computer.

A point scatterer in a basic quality assurance phantom (ATS Laboratories, Inc., Bridgeport, CT) was used as target when studying the vibrations caused by holding the probe with the hand. The speed of sound in the phantom was 1440 m/s, and this was taken into account when calculating the wave number k_0 in (9). A muscle interface of the biceps muscle of a volunteer was used as a target when studying muscle vibrations in the patient. For the muscle recordings the probe was fixed. The wavelength was in this setting 257 μm, and the beam opening angle 2.0 degrees or equivalently the beam width was 2.5 mm at a range of 5 cm.

The power spectrum of each recorded doppler signal recording was estimated using a nonoverlapping periodogram on a signal subset of length 1500 samples windowed with a Hanning window. Using the method of (9), the radial motion of the target was estimated from the doppler signal, and the power spectrum of this motion was also calculated using a nonoverlapping periodogram, and smoothed by zero-padding the signal to length 4096. As an example, Fig. 3 shows the radial motion estimated from the doppler signal from a hand held transducer. The corresponding vibration power spectrum is given in Fig. 4(a).

TABLE I
The Parameters Used When Simulating the Blood and Clutter Signal Power Spectra.

Speed of sound	$c = 1540$ m/s
Muscle vibration amplitude	$a = 25$ μm
Muscle vibration frequency	$f_v = 10$ Hz
Tissue signal power factor	$\alpha^2 = \lvert A(f_0)\rvert = 0$ dB
Blood signal power factor	$\alpha_b^2 = -60$ dB (at 6 MHz)
Ultrasound transducer diameter	$D = 10$ mm
Number of periods in the burst	$N_p = 10$

From the measured signals we got the muscle vibration amplitude and frequency, which were the necessary parameters to simulate the clutter power spectrum in (13). We could then find the minimum blood velocities that are detectable, i.e., the minimum velocities which give a simulated blood power spectrum $P_b(f)$ from (18) that lies above the peaks in the clutter power spectrum $P_c(f)$. Since we know the ultrasound frequency dependency of all the factors involved, we can find the minimum detectable blood velocity as a function of the ultrasound frequency. The frequency dependent attenuation is equal for blood and muscle, so it could be ignored in this case. The parameter values used in the simulations are given in Table I.

IV. Results

Two power spectra of the doppler signal from a fixed point scatterer are shown in Figs. 5(a) and (b). In Fig. 5(a) the probe was fixed, and in Fig. 5(b) the probe was hand held. Notice that the bandwidth increases when the probe is hand held. Figs. 5(c) and (d) show the power spectra of the doppler signal from a relaxed and strained biceps muscle, respectively. Notice the increased bandwidth when the muscle in strained.

The radial displacements were estimated and their power spectra are shown in Fig. 4. Table II lists the results of the recordings; the measured doppler bandwidth, the maximum amplitude and the principal frequency of the estimated displacement signal, and the estimated modulation index.

Using a vibration amplitude 25 μm and a vibration frequency 10 Hz, the clutter power spectrum in (13) was estimated for different ultrasound frequencies. The blood power spectrum of (18) was estimated for each of the ultrasound frequencies, and for varying blood velocities. An example of the two spectra for an ultrasound frequency of 6 MHz is shown in Fig. 6. In Fig. 6(a) the blood velocity is 4.5 mm/s, and in Fig. 6(b) 9.0 mm/s, indicating that the

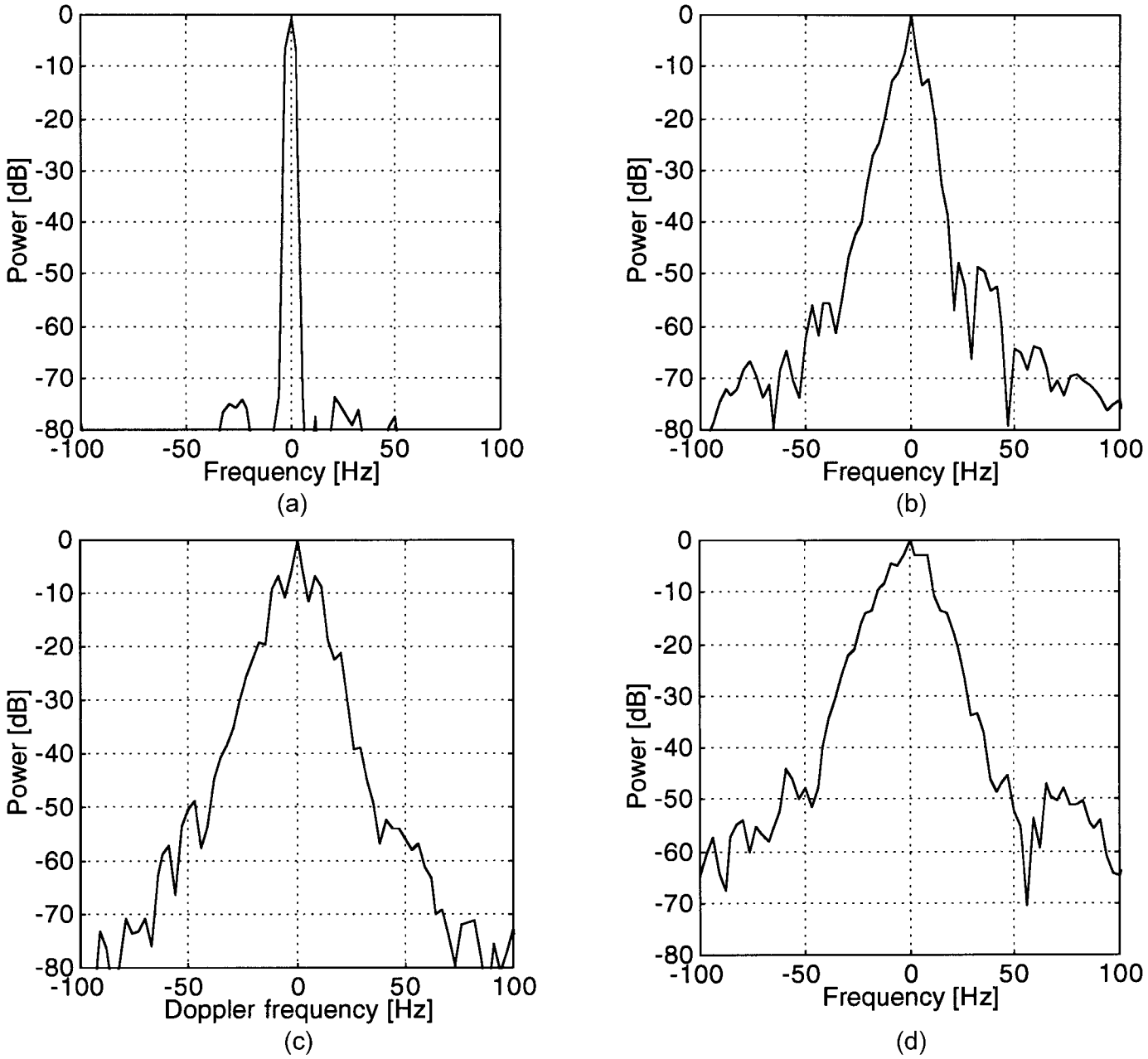

Fig. 5. Doppler spectra from (a) a fixed target using a fixed probe, (b) a fixed target using a hand-held probe, (c) a relaxed biceps muscle using a fixed probe, and (d) a strained biceps muscle using a fixed probe.

TABLE II

ESTIMATED PARAMETERS FROM THE 6 MHz DOPPLER MEASUREMENTS. THE DOPPLER SIGNAL BANDWIDTH IS FOUND FROM THE POWER SPECTRA IN FIG. 5. THE VIBRATION AMPLITUDE IS FOUND AS THE MAXIMUM OF THE DISPLACEMENT SIGNAL ESTIMATED USING (9). THE PRINCIPAL VIBRATION FREQUENCIES ARE FOUND FROM THE POWER SPECTRA OF THE DISPLACEMENT SIGNALS IN FIG. 4. THE MODULATION INDEX IS FOUND FROM (7).

Probe setting	Target	Measured −60 dB Doppler single sided bandwidth [Hz]	Maximum vibration amplitude [μm]	Principal vibration frequency [Hz]	Modulation index, β
Fixed	Fixed point scatterer	2.9	0.12	0	–
Hand held	Fixed point scatterer	59	24	10	1.4
Fixed	Relaxed biceps muscle	47	15	8.1	0.77
Fixed	Strained biceps muscle	95	32	8.1	2.0

TABLE III
LOWEST DETECTABLE BLOOD VELOCITY AT DIFFERENT ULTRASOUND FREQUENCIES FOR THE PARAMETER SETTINGS GIVEN IN TABLE I. THE VELOCITIES ARE GIVEN FOR ULTRASOUND BEAM DIRECTIONS PARALLEL TO THE BLOOD FLOW DIRECTION. THE MODULATION INDEX β IS FOUND FROM (11).

Ultrasound frequency [MHz]	Modulation index, β	Minimum detectable blood velocity [mm/s] at 0 degrees' insonation angle
1	0.20	29
2	0.41	16
4	0.82	8.7
6	1.2	6.4
8	1.6	5.2
10	2.0	4.6
15	3.1	3.5
20	4.1	3.0
30	6.1	2.5
50	10	2.1
100	20	1.7

minimum blood velocity that is detectable is between these values. For each ultrasound frequency the minimum blood velocity was found in the same fashion, and the results are shown in Table III. Notice that, while the modulation index is linearly dependent on the ultrasound frequency, the minimum detectable velocity has a nonlinear relationship to the ultrasound frequency.

V. DISCUSSION

As shown in Figs. 4(a) and (b), low frequency side bands in the doppler signal are introduced when the ultrasound probe is held by the operator. This is caused by the vibrations in the hand and arm muscles of the operator, that impose a vibration on the transducer relative to the phantom target. As shown in Figs. 4(c) and (d), vibrations in the skeletal muscles of a patient also introduce similar side-bands. If both vibration patterns are present during a recording, they add up to a total vibration with expected amplitude equal to $\sqrt{2}$ times the root-mean-square of the two original vibration amplitudes.

Some of the approximations made when developing the theory and when simulating the vibration clutter signal are verified by the experiments. As shown in Table II, the amplitude of the muscle vibrations is much smaller than a wavelength. This means that the approximations leading to (8) are valid. The power spectra in Fig. 4 show that a typical muscle vibration is a band pass signal. By comparing the simulated clutter signal in Fig. 6 and the measured signal in Fig. 5(b) it still seems that simulating a vibration signal using a single frequency is reasonable.

The validity of the low velocity limits presented in Table III is restricted by several conditions. First, when simulating the clutter spectrums, we have assumed an unlimited observation time. For observation times much shorter than the muscle vibration period $1/f_v$, the clutter signal spectrum estimate has only a narrow frequency band around the doppler shift frequency, as described in Section IIA. The blood velocity measurements are then limited to the instantaneous velocity of the vibrating probe or muscle. Second, the effects of vessel wall motion and gross tissue motion have been ignored. When such motion is present, the low velocity limit is the sum of the velocity found in Table III and the velocity of the vessel wall or gross tissue motion, as described in the introduction. Third, as seen in Table I, a specified blood-to-clutter signal level of -60 dB has been used when simulating the blood and clutter spectra. If a higher blood-to-clutter level is obtained, for example by the use of contrast agents, the low velocity limit will be lower. The exact limit for other blood-to-signal levels can be estimated using the method described.

Other publications have shown measurements of blood flow velocities below the limits predicted in Table III. In [18], a 5 MHz doppler technique using no rejection filter and long acquisition time was able to measure velocities down to 1 mm/s in a flow phantom. This is lower than the result predicted in Table III, but muscle vibration clutter signal was not considered or present during the acquisition. Also the blood-to-clutter level was not given, and might have been higher than -60 dB.

VI. CONCLUSIONS

We have found that involuntary skeletal muscle vibrations in the hand of the operator and in the patient itself introduce a phase modulation of the doppler signal. The radial component of the vibration can be found from the phase of the doppler signal. The vibrations introduce low frequency side-bands in the signal and limit the possibility of detecting low velocity blood flow. Our measurements and simulations, assuming -60 dB blood-to-clutter level, indicate that capillary blood flow is not detectable when muscle vibration is present, and will therefore not be visible in velocity and/or power color flow images. The flow in larger vessels like arterioles and small arteries is detectable for ultrasound frequencies higher than 4 MHz.

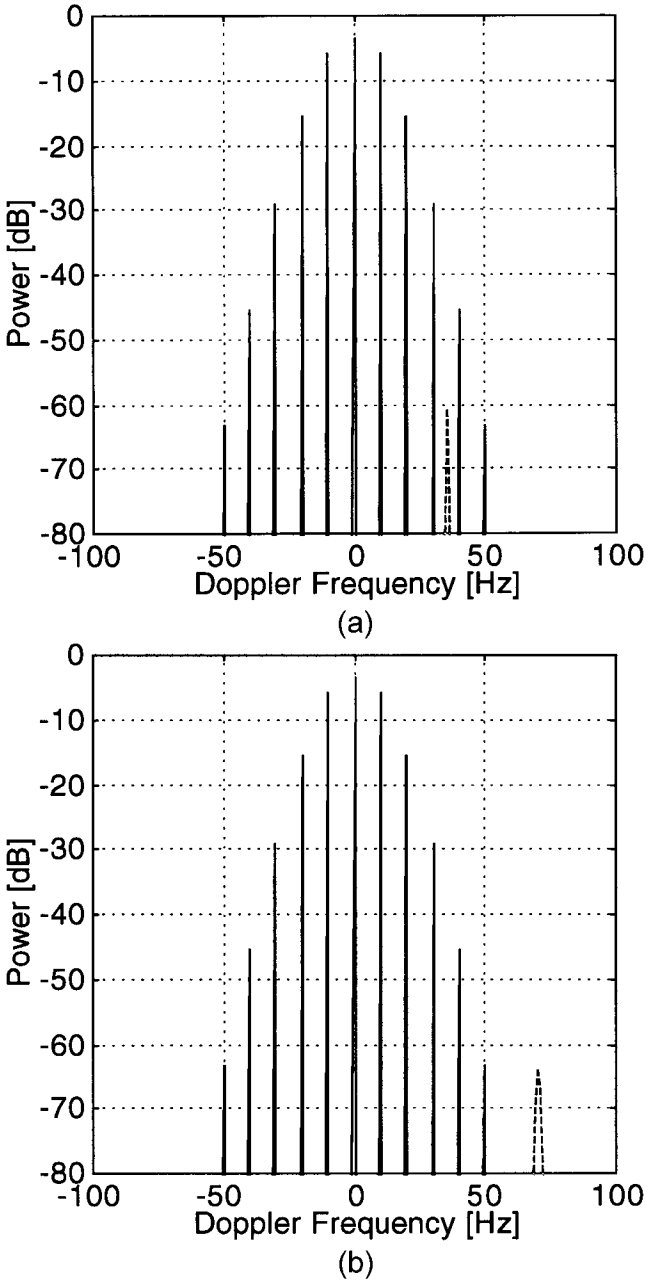

Fig. 6. Simulated doppler signal power spectra from a vibrating scatterer (solid line) and constant blood flow (dashed line), for blood velocities of (a) 4.5 mm/s and (b) 9 mm/s. An ultrasound frequency of 6 MHz was used in the simulation.

Appendix

During the digitizing of the doppler signal, we were not able to avoid high pass filtering of the doppler signal. To estimate the power of the DC component of the doppler signal, the probe was at the end of each recording pulled rapidly away from the target. This caused a shift of the spectrum, so that the high pass filter did not remove any significant amount of the power, and the total power could be calculated by integrating this spectrum. The power of the DC component could then be found from the difference between the calculated total power and the power of the original high pass filtered signal.

To estimate the phase of the DC component, the geometry of the doppler signal in the complex plane can be used. For small modulation indices the complex signal samples lie approximately on a small part of a circle arc. The DC vector is then perpendicular to the tangent of this arc, and the phase can be found as the angle of the vector. From (9) we see that an error in the phase introduces a bias in the amplitude of the estimated radial displacement function.

References

[1] A. J. Vander, J. H. Sherman, and D. S. Luciano, *Human Physiology: The Mechanisms of Body Functions*, 5th ed. New York: McGraw-Hill, 1990.

[2] M. J. Stokes and P. A. Dalton, "Acoustic myography for investigating human skeletal muscle fatigue," *J. Appl. Physiol.*, vol. 71, pp. 1422–1426, 1991.

[3] G. Oster and J. S. Jaffe, "Low frequency sounds from sustained contraction of human skeletal muscle," *Biophys. J.*, vol. 30, pp. 119–128, 1980.

[4] J. Holen, R. C. Waag, and R. Gramiak, "Representations of rapidly oscillating structures on the Doppler display," *Ultrasound Med. Biol.*, vol. 11, pp. 267–272, 1985.

[5] H. Kanai, H. Satoh, K. Hirose, and N. Chubachi, "A new method for measuring small local vibrations in the heart using ultrasound," *IEEE Trans. Biomed. Eng.*, vol. 40, pp. 1233–1241, 1993.

[6] Å. Grønningsæter, "Reduction of acoustic and electronic noise in intravascular ultrasound imaging," Ph.D. thesis, University of Trondheim, 1992.

[7] C. Lentner, "Geigy Scientific Tables," vol. 5, 8th ed. Basel: CIBA-GEIGY Limited, 1990.

[8] S. O. Dymling, H. W. Persson, and G. H. Hertz, Measurements of blood perfusion in tissue using doppler ultrasound," *Ultrasound Med. Biol.*, vol. 17, pp. 433–444, 1991.

[9] A. C. Guyton, "The systemic circulation." *Textbook of Medical Physiology.* Philadelphia: Saunders, 1986, pp. 218–220.

[10] J. Ostergren and B. Fagrell, "Skin capillary blood cell velocity in man. Characteristics and reproducibility of the reactive hyperemia response," *Int. J. Microcirc. Clin. Exp.*, vol. 5, pp. 37–51, 1986.

[11] R. Tepper, Y. Zalel, M. Altaras, G. BenBaruch, and Y. Beyth, "Transvaginal color doppler ultrasound in the assessment of invasive cervical carcinoma," *Gynec. Oncol.*, vol. 60, pp. 26–29, 1996.

[12] W. Lee, J. Chu, C. Huang, M. Chang, K. Chang, and K. Chen, "Breast cancer vascularity: Color doppler sonography and histopathology study," *Breast cancer Res. Treatment*, vol. 37, pp. 291–298, 1996.

[13] A. Fronek, *Noninvasive Diagnostics in Vascular Disease*. New York: McGraw-Hill, 1989.

[14] S. Haykin, *Communication Systems*, 2 ed. New York: Wiley, 1983.

[15] B. Angelsen, *Waves, Signals and Signal Processing in Medical Ultrasonics*. Trondheim: Department of Physiology and Biomedical Engineering, Norwegian University of Science and Technology, 1996.

[16] H. Torp, K. Kristoffersen, and B. Angelsen, "Autocorrelation techniques in color flow imaging. Signal model and statistical properties of the autocorrelation estimates," *IEEE Trans. Ultrason., Ferroelect., Freq. Contr.*, vol. 41, pp. 604–612, 1994.

[17] B. A. J. Angelsen, "A theoretical study of the scattering of ultrasound from blood," *IEEE Trans. Biomed. Eng.*, vol. BME-27, pp. 61–67, 1980.

[18] T.-H. Ting, V. L. Newhouse, and Y. Li, "Doppler ultrasound technique for measuring capillary-speed flow velocities with strong stationary echoes," *Ultrasonics*, vol. 30, pp. 225–231, 1992.

Andreas Heimdal was born in Tønsberg, Norway, in 1969. He received the sivilingeniør (M.S.) degree in electrical engineering from the Norwegian Institute of Technology, University of Trondheim, Norway, in 1993.

He is currently working on a Dr.ing. (Ph.D.) thesis on tissue differentiation based on scatterer movement in ultrasound imaging at the Department of Physiology and Biomedical Engineering, Faculty of Medicine, Norwegian University of Science and Technology, on a scholarship from the Norwegian Research Council. His research interests include ultrasound RF-signal processing for quantification of pysiological parameters.

Hans G. Torp (M'92) was born in Sarpsborg, Norway, in 1953. He received the M.S. and Dr.Techn. degrees from the University of Trondheim, Norway, in 1978 and 1992, respectively.

From 1979 to 1983 he worked at the Division of Automatic Control, SINTEF (The Foundation for Scientific and Industrial Research at the Norwegian Institute of Technology) in Trondheim. Since 1983 he has been working at the Department of Physiology and Biomedical Engineering, Faculty of Medicine, Norwegian University of Science and Technology. He is currently a Research Fellow, holding a stipend from the Norwegian Research Council. His research interests include stochastic signal/image processing with applications in ultrasonic imaging, doppler, and color flow imaging.